David Tomás Sánchez Martínez
Lourdes García Rodríguez
(coordinadores)

Proceedings of the 7th International Seminar on

ORC Power Systems

Editorial Universidad de Sevilla

Proceedings of the 7th International Seminar on

ORC
Power Systems

David Tomás Sánchez Martínez
Lourdes García Rodríguez
(coordinadores)

Proceedings of the 7th International Seminar on

ORC Power Systems

(ORC2023)

4th to 6th
SEPTEMBER
SEVILLE 2023

EDITORIAL UNIVERSIDAD DE SEVILLA

Sevilla, 2024

Colección Actas
Núm.: 91

Review chairs of the 7th International Seminar on ORC Power Systems

Prof. Christoph Wieland (University of Duisburg-Essen) - *Review Chair*
Prof. Sotirios Karellas (National Technical University of Athens) - *Review Co-Chair*
Prof. Teemu Turunen-Saaresti (LUT University) - *Review Co-Chair*
Dr. Diego-César Alarcón-Padilla (Plataforma Solar de Almería - CIEMAT) - *Review Co-Chair*
Dr. Francesco Crespi (Universidad de Sevilla) - *Review Co-Chair*

c/ Porvenir, 27 - 41013 Sevilla.
Tlfs.: 954 487 447; 954 487 451; Fax: 954 487 443
Correo electrónico: info-eus@us.es
Web: https://editorial.us.es

ISBN 978-84-472-2745-7
DOI: https://dx.doi.org/10.12795/9788447227457

Diseño de cubierta y maquetación: los autores

INDEX OF CONTRIBUTIONS

DOI: https://dx.doi.org/10.12795/9788447227457_104

Investigating the application range of ORC power plants for the exploitation of two-phase geothermal resources

Tristan Merbecks[1,2,*], Claudio Pietra[3], Paola Bombarda[1], Martin O. Saar[3], Paolo Silva[1], Dario Alfani[1]

[1] *Politecnico di Milano, Dipartimento di Energia, Via Lambruschini 4, 20157 Milano, Italy*
[2] *ETH Zurich, Department of Earth Sciences Soneggstrasse 5, 8092 Zurich, Switzerland*
[3] *Turboden s.P.a, Via Cernaia 10, 25124, Brescia, Italy*

*Corresponding Author: tristanleonard.merbecks@polimi.it or tmerbecks@ethz.ch

ABSTRACT

The design of a geothermal power plant exploiting a two-phase geothermal resource is a demanding task, due to the fact that different technologies and plant configurations must be considered, as well as the lack of flexible and reliable models for computing the thermophysical properties of geofluids, whose composition and chemistry is highly site-specific.

This study presents a novel thermophysical property modelling framework aimed at modelling any arbitrary single- or two-phase geothermal brine. Recognising the potential synergy of two historically separate fields of research, fluid partition and property modelling, existing partitioning simulators, like Reaktoro, are coupled with high-accuracy thermophysical fluid property computation engines, like CoolProp and ThermoFun. The resultant Python-based framework, GeoProp, is validated against a range of primary and secondary data and will be made available to the public.
Considering a two-phase geothermal resource, the design of direct steam cycles with flash as well as binary geothermal power plants is investigated from a thermodynamic perspective. A parametric study on geofluid composition, i.e. mineral and non-condensable gases (NCG) content, and inlet conditions, i.e. temperature and steam quality, is used to compare the performance and define the application envelope of these two technologies.

1 INTRODUCTION

Geothermal energy is proving to be an attractive and versatile option for grid-scale renewable and dispatchable electricity and heat. Direct steam cycles with flash currently represent the majority of geothermal electricity generation capacity, however binary organic Rankine cycles (ORCs) have allowed the industry to exploit lower enthalpy and otherwise uneconomical geothermal resources.

Binary ORCs have several operational advantages over direct steam cycles (e.g. smaller, cheaper and more durable turbines, closed loop), and in this respect, extending their application envelope is not only of commercial interest but also has the potential to accelerate the adoption of geothermal energy utilization.

While the design, optimisation and operation of ORCs is well understood, the phase behaviour and thermophysical properties of the geothermal fluids represent a key uncertainty for their design, and in particular of the primary heat exchanger, with open-source tools like CoolProp, Reaktoro and ThermoFun only partially providing the required properties. Moreover, the surface handling/reinjection of non-condensable gas (NCG), primarily composed of CO_2, needs to be factored into the techno-economic comparison of direct steam cycles and binary ORCs.

1.1 Objectives

It is in this context that this study aims to:

- present a novel thermophysical property modelling framework for geothermal brines of arbitrary composition, covering a wide range of specific enthalpies and pressures of interest for geothermal applications as well as allowing for the coexistence of aqueous, gaseous, liquid and mineral phases.
- refine the application range of direct steam cycles with flash and binary ORC geothermal power plants for two-phase sources, which are currently predominantly exploited via direct steam cycles.

2 THERMOPHYSICAL PROPERTY MODELLING

A geothermal brine can be regarded as a chemically active system. The constituent species may partition into different phases (e.g. vapour, aqueous, or solid), with some species co-existing in multiple phases (e.g. H_2O[aq] and H_2O[g]), dissociating as they transition into a different phase (e.g. NaCl[s] into Na^+[aq] and Cl^-[aq]), or reacting with each other (e.g. CO_3^{2-}[aq] and H^+[aq] react to HCO_3^-[aq]).

2.1 Theoretical Background

For a system of chemical species (e.g. H_2O[l], Na^+[aq], Cl^-[aq], CO_2[g]), the stable equilibrium state at a pressure, P, and a temperature, T, is the one of minimum Gibbs free energy (e.g. Gyftopoulos & Beretta, 2005). The Gibbs free energy for a given state can be calculated via (1), where G is the Gibbs free energy, $\boldsymbol{n}$ is the vector of species amounts, N is the number of species, n_i is the amount of species i, μ_i is the chemical potential of species i and $\boldsymbol{y}$ is the vector of species mole fractions.

$$G(P, T, \boldsymbol{n}) = \sum_{i}^{N} n_i \mu_i(P, T, \boldsymbol{y}) \tag{1}$$

For a mixture, the chemical potential for each species can be calculated from the species' pure component chemical potential and correcting for interactions with the other species in the system, see (2), where R is the universal gas constant, a_i is the activity of species i and $P°$ and $\boldsymbol{y}°$ refer to the reference pressure and composition, respectively. Conveniently, the partial molar properties of interest, enthalpy, entropy and volume (or density) can be calculated from the chemical potential, see (3) to (5) (Gyftopoulos & Beretta, 2005). 616

$$\mu_i(P, T, \boldsymbol{y}) = \mu_i^{\circ}(T, P^{\circ}, \boldsymbol{y}^{\circ}) + RT \ln a_i(T, P, \boldsymbol{y}) \tag{2}$$

$$h_i(T, P, \boldsymbol{y}) = \left.\frac{d(\mu_i(T, P, \boldsymbol{y})/T)}{d(1/T)}\right|_{P,\boldsymbol{y}} \tag{3}$$

$$s_i(T, P, \boldsymbol{y}) = -\left.\frac{d(\mu_i(T, P, \boldsymbol{y}))}{d(T)}\right|_{P,\boldsymbol{y}} \tag{4}$$

$$v_i(T, P, \boldsymbol{y}) = \left.\frac{d(\mu_i(T, P, \boldsymbol{y}))}{d(P)}\right|_{T,\boldsymbol{y}} \tag{5}$$

2.2 Existing Models

Although the partitioning and property modelling should be in principle the two faces of the same coin, in practice they are treated as two different disciplines in the academic literature and open-source computing frameworks.

For example, partition models (e.g. (Duan & Sun, 2003; Spycher et al., 2003; Spycher & Pruess, 2010) generally focus on the partition of brines and CO_2 mixtures, but do not include thermophysical properties. This is understandable since these models are primarily developed in the context of carbon capture and storage, where the key question is whether the injected CO_2 will dissolve into the brine at in-situ conditions. Similarly, the open-source library CoolProp (Bell et al., 2014) implements a number of equations of state (EOS), which can be used for evaluating the thermophysical properties of pure fluids (e.g. water, carbon dioxide and many hydrocarbons and refrigerants), mixtures of pure fluids and some pseudo-pure/binary fluids (e.g. MITSW for seawater (Sharqawy et al., 2010) or LiBr for lithium bromide (Pátek & Klomfar, 2006) etc.). However, more complex fluids, such as mixtures of pure and pseudo-pure fluids (e.g. seawater with CO_2) or mixtures of pseudo-pure fluids (e.g. seawater and lithium bromide), can currently not be captured.

Reaktoro (Leal, 2015), a unified open-source framework for modelling chemically active systems, pairs many open-source thermodynamic databases, like SUPCRT98 or SUPCRTBL, and activity models with powerful and scalable optimisation algorithms. Although the thermophysical property predictions are generally accurate for aqueous systems, they lack accuracy for vapour-liquid systems, see Figure 1 and Figure 2. The observed deviations can be attributed to the underlying databases prescribing non-standard EOS to be used for important vapour species like H_2O[g] and CO_2[g].

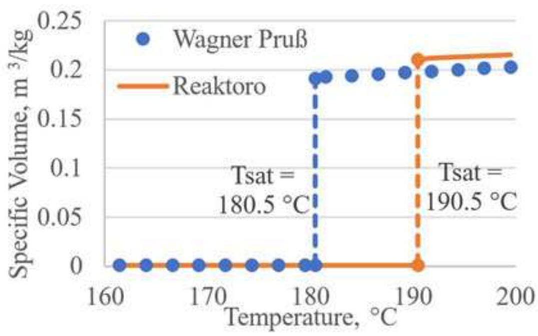

Figure 1: The specific volume of a system consisting of H_2O[aq] and H_2O[g] at a pressure of 10 bar as a function of temperature. The dashed lines indicate the saturation temperatures.

617

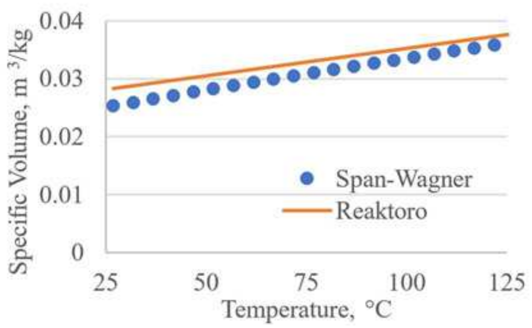

Figure 2: The specific volume of a chemically active system consisting of CO_2[aq] at a pressure of 20 bar as a function of temperature.

3 GeoProp

Leveraging the strengths of the aforementioned tools, a modularised approach was chosen, see Figure 3, – the resultant model, GeoProp, can model geofluids with arbitrary composition over a wide range of conditions.

After defining the main geofluid constituents, the selected partition model, by default Reaktoro, equilibrates the fluid at the specified temperature and pressure. GeoProp then sorts the equilibrium species into the corresponding phases (i.e. aqueous, gaseous and mineral) and passes them to CoolProp and ThermoFun (Miron et al., 2021), whichever is more appropriate, for estimating the thermophysical properties. GeoProp then aggregates the thermophysical properties of the individual phases using a simple mass-based mixing rule. GeoProp is implemented in Python and will available to the public.

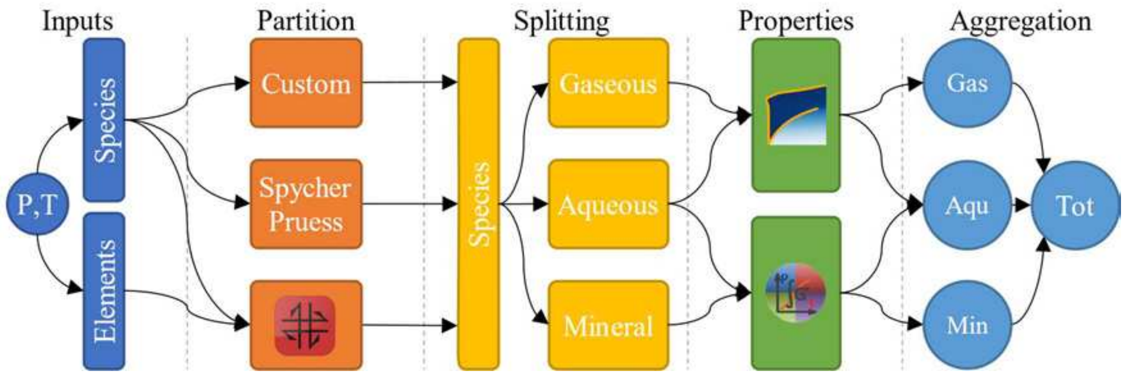

Figure 3: The architecture of the thermophysical property model for brines and NCG.

GeoProp was validated using the MITSW and LiBr models, for seawater and lithium bromide solution, respectively, implemented in CoolProp, as well as published data for three fluids from a geothermal field near Makhackala, Russia, (Abdulagatov et al., 2016). The fluids were recreated in GeoProp, partitioned, to determine the equilibrium compositions, and the thermophysical properties evaluated. GeoProp reproduced the density of the different fluids to within 3 %, slightly outperforming the prediction by Aspen Plus V11's ELECNRTL model, see Figure 4. All models predicted the specific enthalpy to within 1 %, see Figure 5.

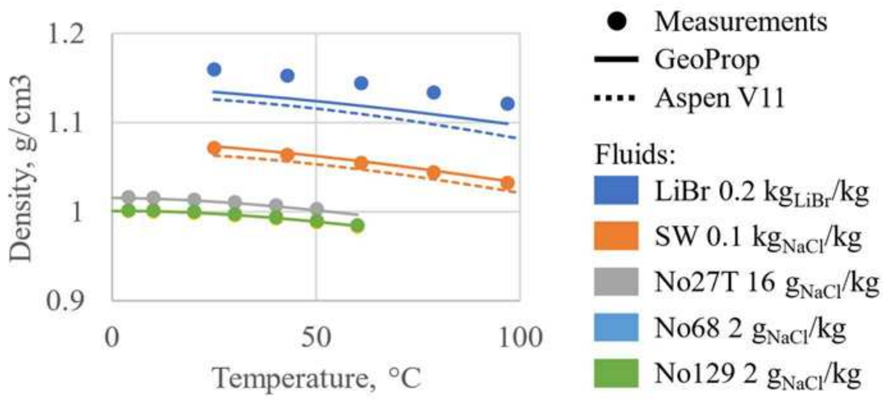

Figure 4: The density of various brines as a function of temperature at 1 bar pressure. Dots represent "measured" data and lines represent property models.

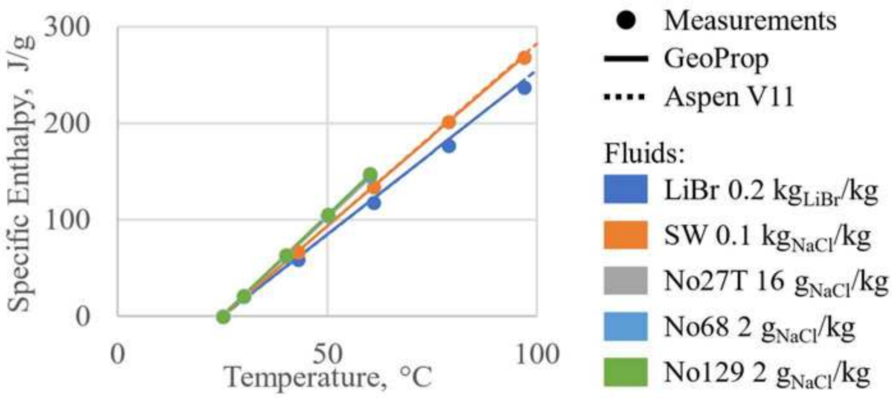

Figure 5: The specific enthalpy of various brines as a function of temperature at 1 bar pressure. The reference temperature is 25 °C. Dots represent "measured" data and lines represent property models.

4 TECHNOLOGY MAP

4.1 Geothermal Sources

Primarily two-phase geothermal sources were considered, with wellhead temperatures ranging between 100 °C and 200 °C and steam quality, defined in (6), ranging between 0 to 0.5. Heat losses between the wellhead and the plant inlet were assumed to be insignificant and therefore neglected. The brine salinities, defined in (7) as NaCl, and NCG content, defined in (8) as CO_2, range between 0 to 0.3 kg_{NaCl}/kg_{H2O} and 0 to 0.03 kg_{CO2}/kg_{H2O} respectively.

$$x = \frac{\dot{m}^V_{H_2O}}{\dot{m}^L_{H_2O} + \dot{m}^V_{H_2O}} \tag{6}$$

$$sal = \frac{\dot{m}_{Salts}}{\dot{m}^L_{H_2O} + \dot{m}^V_{H_2O}} \tag{7}$$

$$NCG = \frac{\dot{m}_{NCG}}{\dot{m}^L_{H_2O} + \dot{m}^V_{H_2O}} \tag{8}$$

While a unit geofluid mass rate could be considered for the power plant simulations, this has the undesirable effect of artificially reducing the power plants' performance as the effective inlet heat rate is lower due to the lower specific heat capacities of salinity and NCG compared to water. Instead, a unit combined mass rate of liquid water and steam is assumed for all cases to which the mass rates of salinity and NCG are added, see (9).

$$\dot{m} = \dot{m}^L_{H_2O} + \dot{m}^V_{H_2O} + \dot{m}_{Salts} + \dot{m}_{NCG} \qquad \text{where, } \dot{m}^L_{H_2O} + \dot{m}^V_{H_2O} = 1 \text{ kg/s} \tag{9}$$

619

4.2 Power Plant Configurations

Two power plant configurations are considered, 1) a direct single flash steam cycle and 2) a binary ORC. In a direct steam cycle only the vapour portion of the geofluid is utilised and subsequently expanded in a turbine, see Figure 6. On the other hand, in a binary ORC the geofluid merely serves as a heat source to vaporise a secondary fluid, which is then expanded in a turbine similarly to the direct steam cycle, see Figure 7. This allows exploiting the heat contained within both the vapour as well as the liquid phase.

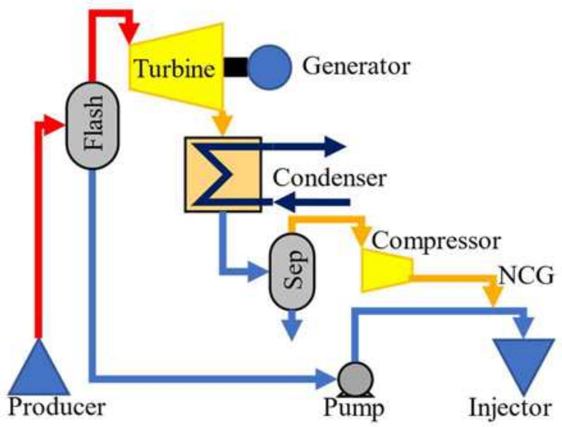

Figure 6: Direct steam cycle geothermal power plant.

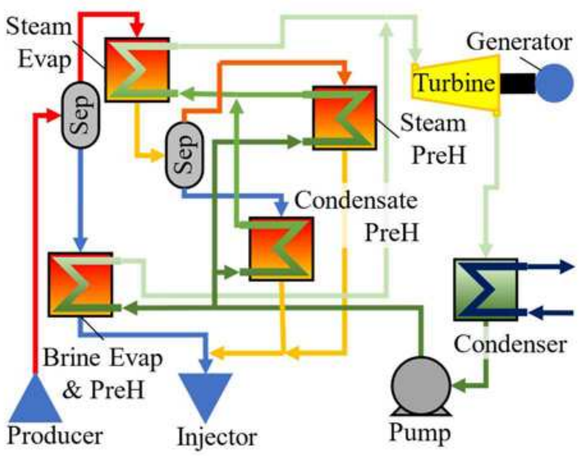

Figure 7: Binary ORC geothermal power plant.

Both power plants are subject to the same boundary conditions:

- Geofluid composition, inlet temperature, pressure and steam quality
- Heat is rejected into the surrounding environment at a temperature of 25 °C
- Geofluid enters and exits the power plant at the same pressure – this is to penalise for NCG handling to ensure that it is not released into the atmosphere but instead reinjected into the formation.
- Geofluid re-injection temperature is not constraint, as scaling is assumed to be negligible.

The specific net power output from the power plant, defined in (10), will be used to judge which performs better for a set of boundary condition.

$$\dot{w}_{net} = \frac{\dot{W}_{turbine} - \dot{W}_{pump} - \dot{W}_{repressurisation}}{\dot{m}^L_{H_2O} + \dot{m}^V_{H_2O}} \tag{10}$$

4.3 Model Description

For the direct steam cycle:

- The net power is optimised by adjusting the flash temperature/pressure, increasing the vapour mass rate while sacrificing specific enthalpy drop across the turbine; the pressure of the liquid fraction is consequently also decreased by the flash process.
- The stream exiting the turbine is then cooled to 30 °C and then separated into a liquid stream and a NCG stream. All outlet streams, i.e. the liquid stream from the flash chamber, the condensate stream and the NCG stream, must then be repressurised to the inlet pressure so that they can be reinjected into the reservoir.
- Given the bell-shaped vapour dome of water in the T-s (temperature-specific entropy) diagram, the turbine efficiency is corrected for liquid drop out using the empirical Baumann Rule, see (11), where $\eta^{wet}_{turbine}$ is the turbine wet efficiency, $\eta^{dry}_{turbine}$ is the turbine dry efficiency, assumed to be 85 % (DiPippo, 2016), and x_{in} and x_{out} are the mole-based vapour fraction at the turbine inlet and outlet respectively.

620

$$\eta^{wet}_{turbine} = \eta^{dry}_{turbine} \frac{(x_{in} + x_{out})}{2} \tag{11}$$

For the binary ORC:

- The incoming geofluid is split into a liquid and vapour stream with each stream being used to pre-heat and evaporate the cycle working fluid. The vapour stream is further split into a vapour and condensate following the vapour powered evaporator.
- The net power is optimised by adjusting evaporation and condensation temperature/pressure and the working fluid mass flow rates, while ensuring that the minimum approach temperatures do not fall below 5 °C in liquid dominated and 10 °C in vapour dominated heat exchangers. Moreover, the vapour quality at the vapour evaporator outlet should be above 0.75.
- Iso-butane, n-butane, iso-pentane, n-pentane and cyclopentane were considered as ORC working fluids.
- The simulations were run in Aspen Plus V11.

4.4 Case 1: Pure Water

To establish a base case, the two power plants were simulated in Aspen Plus V11 for a geofluid modelled as pure water for inlet temperatures and steam quality ranging between 100 °C to 200 °C and 0 to 0.5 respectively. The results are shown in Figure 8, Figure 9 and Figure 10. The key observations are:

- The investigated ORC configurations thermodynamically outperform the direct steam cycles at any temperature for saturated liquid sources. For inlet temperatures above 150 °C, the ORC configurations begin to outperform the direct steam cycles at increasingly higher steam quality.

- All ORC working fluids perform similarly poorly at lower temperatures (up to 150 °C), which can likely be attributed to the critical temperatures of the selected working fluids being too high. Isobutane and n-butane appear the most favourable working fluids for the conditions studied.
- Cross-over of isobutane and n-butane in Figure 9 can be attributed to the vapour heated branch becoming vapour fraction constraint (i.e. the vapour quality in the vapour evaporator outlet reaches the limit of 0.75), limiting the amount of working fluid that can be evaporated.

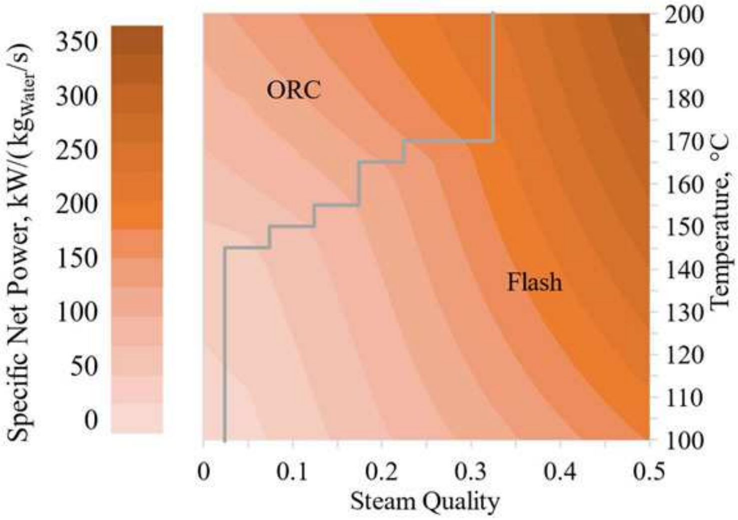

Figure 8: Maximum specific net power from a geofluid of pure water as a function of inlet temperature and steam quality. The grey line indicates the performance boundary between binary ORC and direct steam cycles.

621

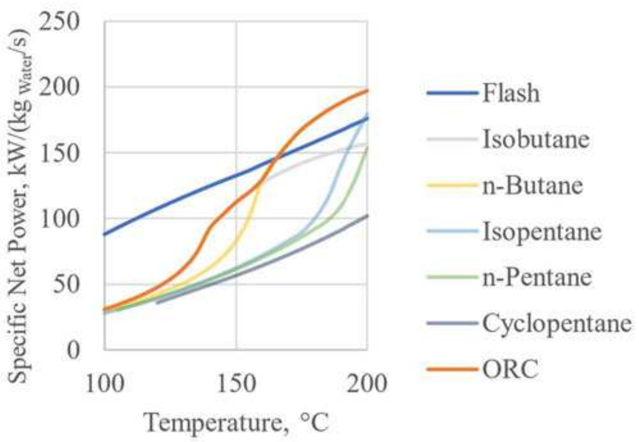

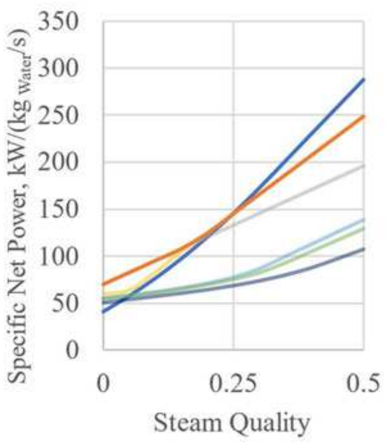

Figure 9 Specific net power from a geofluid of pure water as a function of inlet temperature and a steam quality of 0.25 for a direct steam cycle and binary ORC plant using various working fluids.

Figure 10 Specific net power from a geofluid of pure water as a function of steam quality and an inlet temperature 165°C for a direct steam cycle and binary ORC plant using various working fluids.

4.5 Salinity and NCG

In reality geofluids are not only comprised of pure water, but may also carry dissolved minerals and NCG. The presence of such impurities alters the geofluid's phase behaviour and thermophysical properties compared to pure water, the magnitude of deviations being strongly related to the effective salinity, see (12), and effective NCG content, see (13), and has implications for the performance of direct steam and binary ORC power plants.

$$sal_{eff} = \dot{m}_{NaCl} \Big/ \dot{m}^{L}_{H_2O} \tag{12}$$

$$NCG_{eff} = \dot{m}_{NCG} \Big/ \dot{m}^{V}_{H_2O} \tag{13}$$

Perhaps most consequential is their effect on the geofluid saturation pressure. Considering a geofluid comprised of H_2O[aq], Na^+[aq], Cl^-[aq] and H_2O[g], the presence of the Na^+[aq], Cl^-[aq] causes a reduction in chemical potential of the H_2O[aq], meaning that mixture prefers to be in the liquid state and thus the saturation pressure is reduced, see Figure 11. Similarly, for a geofluid comprised of H_2O[aq], H_2O[g] and CO_2[g], the fluid prefers to be in the gaseous state and hence the saturation pressure increases.

The change in saturation pressure is particularly important for direct steam cycles, as, for example in the case of high salinity, impedes the ability to optimise flash temperature/pressure and reduces net power. Specifically, a geofluid with an effective salinity of 0.3 kg_{NaCl}/kg_{H2O}, the saturation pressure is reduced from 10 bar to 8 bar.

Salinity and NCG also affect the geofluid's thermophysical properties, such as the specific enthalpy or specific heat capacity. Changes can primarily be attributed to both salts and NCG having far lower heat capacity than pure water and to a smaller extent to the reduction in species chemical potential, although this is more significant for higher concentrations of salts and NCG. That being said, the heat flow is relatively unchanged compared to pure water, see Figure 12. This suggests that, assuming the total mass rate scales with the mass rate of impurities, the performance of the binary ORC is only weakly affected.

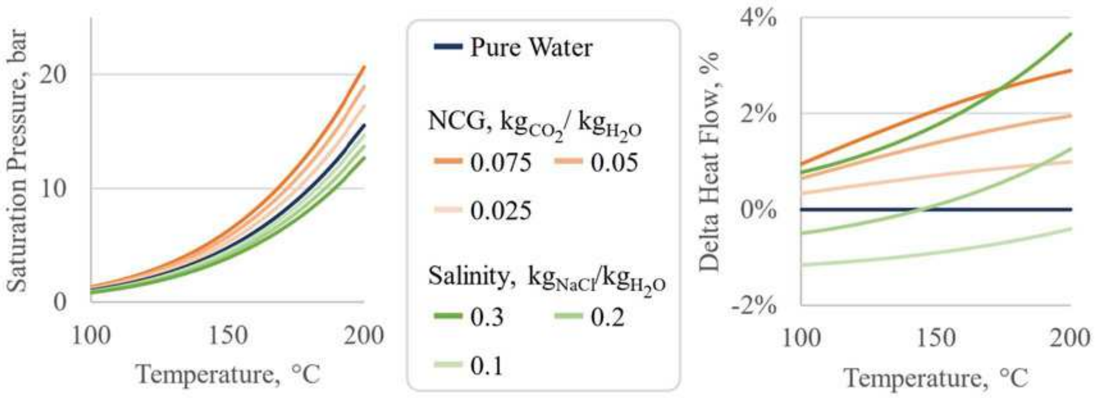

Figure 11: Geofluid saturation pressure as a function of temperature for a range of effective salinity and NCG content.

Figure 12: Deviation of liquid and vapour heat flow from pure water/steam for a range of effective salinity and NCG content, at a steam quality of 0.1, as a function of temperature. The reference conditions are 25 °C and 1 bar.

4.6 Case 2: Salinity and NCG

To investigate the effect of impurities, the two power plants were simulated in Aspen Plus V11 for an inlet temperature of 150 °C and steam quality of 0.1 for geofluid with salinity and NCG content ranging between 0 to 0.2 kg_{NaCl}/kg_{H2O} and 0 to 0.03 kg_{CO2}/kg_{H2O} respectively, see Figure 13 and Figure 14. The key observations were:

- Salinity does not significantly affect the performance of direct steam cycles or ORCs.
- NCG content primarily impacts the performance of direct steam cycles due to the additional compression requirements to reinject the NCG.
- ORCs begin to thermodynamically outperform direct steam cycles at about 0.015 kg_{CO2}/kg_{H2O} for any salinity studied.

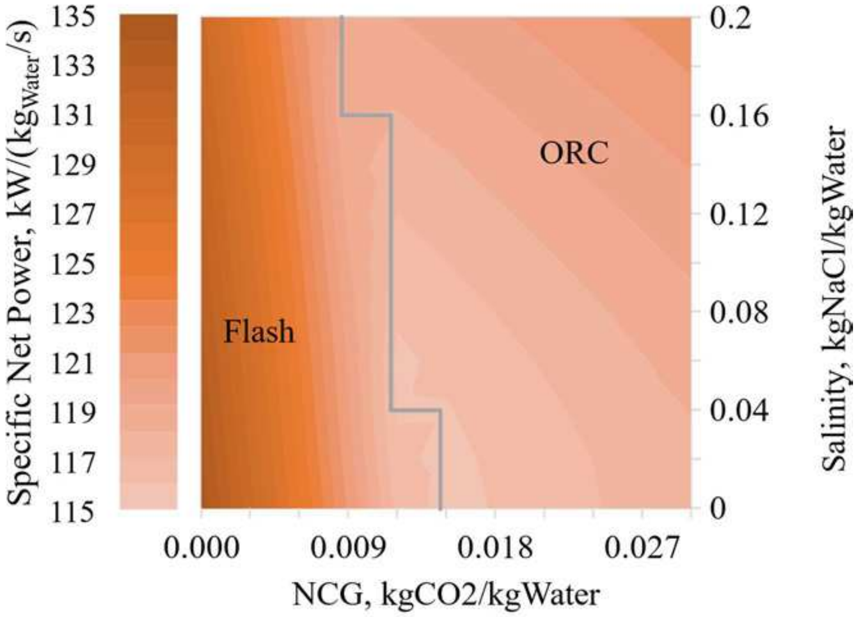

Figure 13: Maximum specific net power from a direct steam cycle or a binary ORC as a function of salinity and NCG content. Inlet temperature is 150 °C and a steam quality of 0.25

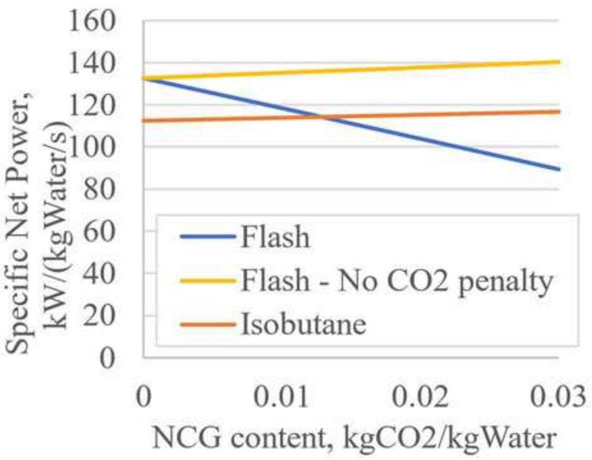

Figure 14: Specific net power as a function of NCG content. Inlet temperature is 150 °C, steam quality is 0.25 and salinity is 0.0 kg_{NaCl}/kg_{H2O}.

623

5 Conclusions

The thermophysical property modelling framework couples existing partitioning and property models, and while the current capabilities for single phase brines are promising, further work is required for handling two-phase geofluids to the same degree. The Python-based framework will in time be made available to the public.

Simulations of geothermal power plants showed that ORCs can thermodynamically outperform direct steam cycles for inlet steam quality as high as 0.3, provided an appropriate working fluid has been selected - isobutane and n-butane were found to be thermodynamically promising working fluids.
The presence of impurities in the geofluid such as salts and NCG does not significantly affect the heat flow entering the power plant, and in turn the turbine power. That being said, NCG compression for reinjection reduced the net power of direct steam cycles significantly, rendering binary ORCs thermodynamically favourable for NCG content as low as 0.01 kg_{CO2}/kg_{H2O}.

6 References

Abdulagatov, I. M., Akhmedova-Azizova, L. A., Aliev, R. M., & Badavov, G. B. (2016). Measurements of the density, speed of sound, viscosity and derived thermodynamic properties of geothermal fluids from south Russia Geothermal Field. Part II. *Applied Geochemistry*, *69*, 28–41. https://doi.org/10.1016/j.apgeochem.2016.04.003

Bell, I. H., Wronski, J., Quoilin, S., & Lemort, V. (2014). Pure and Pseudo-pure Fluid Thermophysical Property Evaluation and the Open-Source Thermophysical Property Library CoolProp. *Industrial & Engineering Chemistry Research*, *53*(6), 2498–2508. https://doi.org/10.1021/ie4033999

DiPippo, R. (2016). *Geothermal Power Plants* (4th ed.). Butterworth-Heinemann. https://doi.org/10.1016/C2014-0-02885-7

Duan, Z., & Sun, R. (2003). An improved model calculating CO2 solubility in pure water and aqueous NaCl solutions from 273 to 533 K and from 0 to 2000 bar. *Chemical Geology*, *193*(3–4), 257–271. https://doi.org/10.1016/S0009-2541(02)00263-2

Gyftopoulos, E. P., & Beretta, G. P. (2005). *Thermodynamics: Foundations and Applications*. Dover Publications.

Leal, A. M. M. (2015). *Reaktoro: An open-source unified framework for modeling chemically reactive systems.* (No. V2). https://reaktoro.org

Miron, G. D., Kulik, D., Leal, A., & Dmytrieva, S. (2021). ThermoFun: C++/Python code to fetch standard thermodynamic data from ThermoHub database. *Goldschmidt2021 Abstracts*. https://doi.org/10.7185/gold2021.4489

Pátek, J., & Klomfar, J. (2006). A computationally effective formulation of the thermodynamic properties of LiBr–H2O solutions from 273 to 500K over full composition range. *International Journal of Refrigeration*, *29*(4), 566–578. https://doi.org/10.1016/j.ijrefrig.2005.10.007

Sharqawy, M. H., Lienhard, J. H., & Zubair, S. M. (2010). Thermophysical properties of seawater: a review of existing correlations and data. *Desalination and Water Treatment*, *16*(1–3), 354–380. https://doi.org/10.5004/dwt.2010.1079

Spycher, N., & Pruess, K. (2010). A Phase-Partitioning Model for CO2–Brine Mixtures at Elevated Temperatures and Pressures: Application to CO2-Enhanced Geothermal Systems. *Transport in Porous Media*, *82*(1), 173–196. https://doi.org/10.1007/s11242-009-9425-y

Spycher, N., Pruess, K., & Ennis-King, J. (2003). CO2-H2O mixtures in the geological sequestration of CO2. I. Assessment and calculation of mutual solubilities from 12 to 100°C and up to 600 bar. *Geochimica et Cosmochimica Acta*, *67*(16), 3015–3031. https://doi.org/10.1016/S0016-7037(03)00273-4

624

7 ACKNOWLEDGEMENTS

This project has received funding from the European Union's Horizon 2020 research and innovation programme under the Marie Skłodowska-Curie grant agreement No 956965.

8 NOMENCLATURE

a	Activity	$(-)$	$\dot{w}$	specific work rate	(kW s/kg)
G	Gibbs free energy	(kJ)	x	steam quality	$(-)$
h	specific enthalpy	(kJ/mol)	y	mol fraction	$(-)$
$\dot{m}$	mass rate	(kg/s)	μ	chemical potential	(kJ/mol)
n	amount	(mol)	η	efficiency	$(-)$
NCG	NCG content	(kg_{CO2}/kg_{H2O})			
P	Pressure	(Pa)		**Subscript**	
s	specific entropy	(kJ/mol/K)	i	species index	
sal	salinity	(kg_{NaCl}/kg_{H2O})			
T	Temperature	(K)		**Superscript**	
v	specific volume	(m^3/mol)	L	liquid phase	
$\dot{W}$	Work rate	(kW)	V	vapour phase	

9 Appendix A

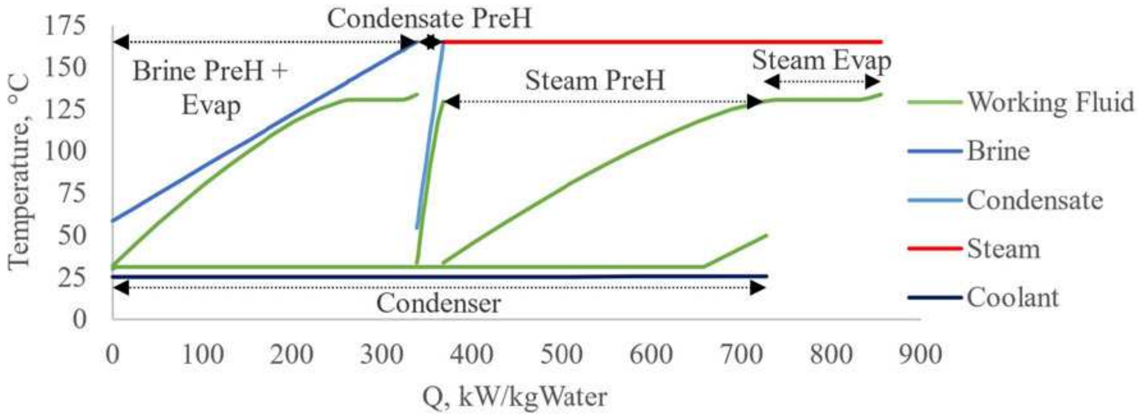

Figure 15 T-Q diagram of the binary ORC plant operating under an inlet temperature of 165 °C and a steam quality of 0.25.

10 Appendix B

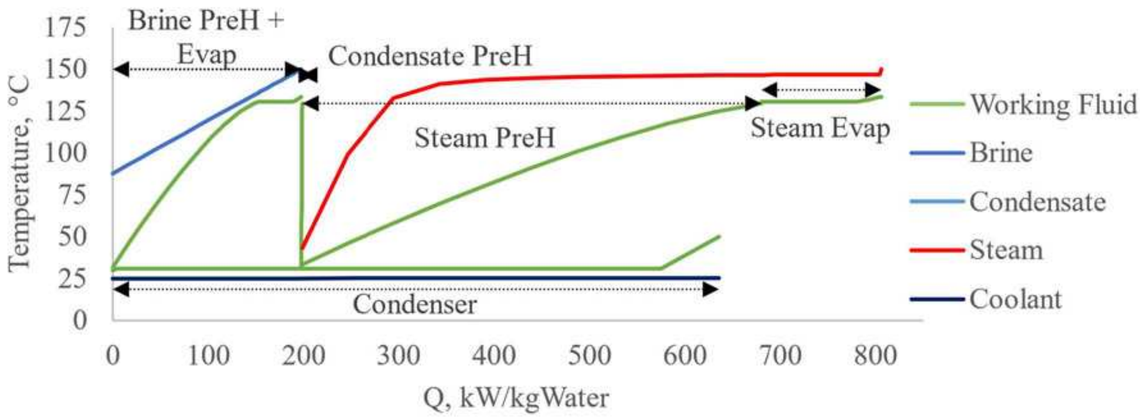

Figure 16 T-Q diagram of the binary ORC plant operating under an inlet temperature of 150 °C, a steam quality of 0.25, salinity of 0.1 kg_{NaCl}/kg_{Water} and NCG of 0.015 kg_{CO2}/kg_{Water}.

625

This book contains the compilation of works contributed to the *7th International Seminar on Organic Rankine Cycle Power Systems* (ORC 2023), held in Seville between the 4th and 6th of September 2023. The event was hosted by Universidad de Sevilla on behalf of the Knowledge Centre on Organic Rankine Cycle Technology (KCORC), incorporated in The Netherlands.

The ORC conference, organized biennially, stems as the only conference that is specific to ORC technology, therefore gathering a diverse community whose affiliation spans across all the interested stakeholders, not only in this particular technology but also and in a broader context, in the energy transition. Original equipment manufacturers, professional associations, end-users, investors, policy makers, academics, scientists feel at home at ORC 2023.

The almost 100 proceedings in this book cover a wide variety of topics, from fundamentals to system integration through component design, accounting for thermodynamic performance as well as component design. In addition to this, and as a new track in 2023, works on heat pump technology were also accepted in order to raise awareness of the strong ties between both technologies, specifically in energy storage applications.

This book provides an excellent overview of the current maturity of power systems based on Organic Rankine Cycle technology for applications as diverse as geothermal and waste heat recovery in industry or downstream of other prime movers (e.g., marine applications). It is also an excellent source of information to understand the current challenges faced by the technology, stemming from a very competitive market and increasingly stringent environmental regulations.

The organizers of ORC 2023 hope that the reader finds this work as exciting as the attendees to the conference and, maybe, make the decision to join the 8th edition to the conference in 2025.

KCORC
KNOWLEDGE CENTER
ORGANIC RANKINE CYCLE

eus EDITORIAL
UNIVERSIDAD DE SEVILLA